A Traffic Model with Junction Constraints for Smart Cities Development

Sabrina Francesca Pellegrino(✉)

Dipartimento di Management, Finanza e Tecnologia,
Università LUM Giuseppe Degennaro, S.S. 100 Km 18,
Casamassima, 70010 Bari, Italy
pellegrino@lum.it

Abstract. Good environmental quality is the foundation for a good quality of life. Technologies of Smart Cities can adequately support the path of sustainability in urban areas and thus compete to raise the quality of life of citizens. In particular, sustainable urban development concept can be characterized in terms of CO2 emissions. In order to address sustainable urban development, management and modeling traffic jam is a primary issue. We propose a mathematical model based on hyperbolic scalar conservation laws with non-local point constraint at the interface and a finite volume scheme to reproduce the capacity drop phenomenon at a road merge. We call capacity drop the situation in which the outflow through the junction is lower than the receiving capacity of the outgoing road, as too many vehicles trying to access the junction from the incoming roads hinder each other. The capability of representing such phenomenon by means of a non-local model allow us to obtain more accurate and detailed information by traffic data provided by sensors which can be used to propose a strategy to manage traffic flow near crossroads and to reduce the congestion in urban setting.

Keywords: Non-local point constraints · Traffic jam · Capacity drop · Smart cities · Sustainability

1 Introduction

In recent years, traffic related problems such as congestion and traffic jams have become a major issue in the cities all around the world and the increasing demand of mobility imposes the need of efficient traffic management solutions. This gave birth to a large number of traffic theories and mathematical models formulated with the aim of understanding and developing optimal transport networks with minimal congestion problems.

Supported by GNCS of Istituto Nazionale di Alta Matematica, by PRIN 2017 "Discontinuous dynamical systems: theory, numerics and applications" and by Regione Puglia, "Programma POR Puglia 2014/2020-Asse X-Azione 10.4 Research for Innovation-REFIN - (D1AB726C)".

© The Author(s), under exclusive license to Springer Nature Switzerland AG 2022
O. Gervasi et al. (Eds.): ICCSA 2022 Workshops, LNCS 13382, pp. 157–172, 2022.
https://doi.org/10.1007/978-3-031-10592-0_13

Managing urban expansion effectively is a global priority, especially in light of growing concerns about climate change. Many cities currently lack the necessary infrastructure to meet the travel needs of their citizens. The intelligent transport systems of the future will have to have less impact on emissions and more efficient and sustainable in terms of energy.

Smart city is a wide concept with connections to physical infrastructures and social factors [3,23]. One of the main aspects of smart cities is traffic control: indeed this issue is strictly related with pollution and economic problems, as businesses suffer from delivery delays and lost productivity and as a consequence, all of these aspects diminishes the city's quality of life.

Smart cities make use of technologies, such as sensors, camera and routers to dynamically alert riders and adjust control mechanisms [4,12,16].

Current trends for traffic control are based on the use of smart traffic lights and signals. From a mathematical point of view, these strategies can be thought as external controls [1,18]. However, most traffic signals are preprogrammed and do not support real-time conditions.

A different approach to deal with these problems is based on the implementation of non-local techniques. In fact, the use of non-local point constraints allows us to have a more realistic representation of the transient behavior between congested traffic and free flow [2,7]. Moreover, from a mathematical point of view, the introduction of a non-local constraint is largely adopted in different contexts in order to have a consistent behavior near discontinuities or interfaces, see for instance [5,6,13–15,20].

Macroscopic traffic models are typically based on systems of conservation laws and describe traffic flow in terms of density of vehicles and average velocity.

The main purpose of the paper is to summarize a non-local approach to model traffic jam and to reproduce the capacity drop phenomenon at a road merge proposed in [7,17,19,22]. This phenomenon expresses the fact that the outflow of a traffic jam is significantly lower than the maximum achievable flow at the same location, as too many vehicles trying to access the junction from the incoming roads hinder each other. More precisely, if the demand is higher than the maximum flow that can pass through the junction at a certain time, a congestion is formed. Empirical observations show that whenever a traffic jam occurs, the maximum outflow that materializes, called discharge flow, may be lower than the receiving capacity of the outgoing road. The capacity drop can then be defined as the difference between these two values, i.e. the receiving capacity and the discharge flow.

To model the capacity drop we introduce a non-local point constraint at junction which maximizes the vehicular passing flow. Additionally, we describe a numerical method based on the implementation of a finite volumes scheme and validate its performance by comparison with explicit solutions. Our tests make evidence that non-local point constraint allows for a more regular transition between capacity drop and capacity recovery, without putting control strategies into practice.

Indeed, non-local models can improve the results of the sensor's revelations: instead of evaluate the vehicles density in a fixed location, sensors could provide an averaged value in a suitable interval in real-time.

The paper is organized as follows. Section 2 describes the proposed methodology used to model and manage the traffic in presence of a crossroad. In particular, Sect. 2.1 briefly introduces the basic notation, describes the proposed non-local model for the capacity drop representation on a road network and outlines the main properties of the non-local model. While, Sect. 2.2 is devoted to the description of the finite volumes scheme. In Sect. 3 we present and discuss the numerical results. More precisely, we validate the finite volumes scheme and show the capability of the model to provide a hint to manage traffic at crossroads. Finally, Sect. 4 concludes the paper.

2 Methodology

The strategy we propose to represent the capacity drop at crossroads consists in the implementation of a nonlocal point constraint at a junction of a road merge. In the next sections, we briefly recall the basic notations and introduce the mathematical background for the construction of the model and then we describe a constrained finite volume scheme used for the simulations.

2.1 The Non-local Model for the Capacity Drop Representation

We consider a road network consisting of two incoming and one outgoing roads and a junction. The incoming roads are parametrized by the negative real line, here denoted by $\Omega_i = (-\infty, 0]$ for $i \in \mathsf{I} = \{1, 2\}$, while the outgoing one is parametrized by the positive real line, denoted by $\Omega_3 = [0, \infty)$. In this way the junction is located at $x = 0$. For simplicity we fix the index $h \in \mathsf{H} = \{1, 2, 3\}$ and we denote the network by $\mathcal{N} = \Pi_{h\in\mathsf{H}}\Omega_h$.

On each road we describe the traffic evolution by the Lighthill-Whitham-Richards model [11,21], namely by a scalar conservation law of the form

$$\partial_t \rho_h + \partial_x f_h(\rho_h) = 0, \qquad t > 0, \quad x \in \Omega_h, \tag{1}$$

where ρ_h is the density of vehicles and f_h is the flux along the h-th road. We fix the initial conditions

$$\rho_h(0, x) = \rho_{h,0}(x), \qquad x \in \Omega_h, \tag{2}$$

and we assume they are in $L^1 \cap \mathrm{BV}(\Omega_h; [0, \rho_{\max}])$. Moreover, we suppose that the roads have a common maximal density $\rho_{\max}$, admit a maximum point $\rho_{h,c}$, for $h = 1, 2, 3$, and finally, we require the conservation of the number of vehicles across the junction

$$f_3(\rho_3(t, 0^+)) = f_1(\rho_1(t, 0^-)) + f_2(\rho(t, 0^-)), \tag{3}$$

for a.e. $t > 0$.

We use the following definition of weak solution on the network.

Definition 1. *The vector function* $\boldsymbol{\rho} = (\rho_1, \rho_2, \rho_3)$*, where* $\rho_h : (0,\infty) \times \Omega_h \to [0, \rho_{\max}]$*,* $h \in \mathsf{H}$*, is a* weak solution *to* (1)–(2)*,* $h \in \mathsf{H}$*, in the network if*

- $\rho_h \in \mathcal{C}^0((0,\infty); L^1(\Omega_h; [0,\rho_{\max}])) \cap \mathrm{BV}_{\mathrm{loc}}((0,\infty) \times \Omega_h; [0,\rho_{\max}])$*,* $h \in \mathsf{H}$*;*
- *for* $i \in \mathsf{I}$*,* ρ_i *is a weak entropy solution to* (1)–$(2)_{h=i}$*, namely for every* $c \in [0,\rho_{\max}]$ *and every nonnegative test function* $\phi \in \mathcal{C}^\infty(\mathbb{R} \times (-\infty, 0); \mathbb{R})$ *with compact support*

$$\int_0^\infty \int_{\Omega_i} \Big(|\rho_i - c|\, \partial_t \phi + \operatorname{sign}(\rho_i - c)\big(f_i(\rho_i) - f_i(c)\big)\partial_x \phi \Big)\, \mathrm{d}x\, \mathrm{d}t + \int_{\Omega_i} |\rho_{i,0}(x) - c|\, \phi(0,x)\, \mathrm{d}x \geq 0;$$

- ρ_3 *is a weak entropy solution to* (1)–$(2)_{h=3}$*, namely for every* $c \in [0,\rho_{\max}]$ *and every nonnegative test function* $\phi \in \mathcal{C}^\infty(\mathbb{R} \times (0,\infty); \mathbb{R})$ *with compact support*

$$\int_0^\infty \int_{\Omega_3} \Big(|\rho_3 - c|\, \partial_t \phi + \operatorname{sign}(\rho_3 - c)\big(f_3(\rho_3) - f_3(c)\big)\partial_x \phi \Big)\, \mathrm{d}x\, \mathrm{d}t + \int_{\Omega_3} |\rho_{3,0}(x) - c|\, \phi(0,x)\, \mathrm{d}x \geq 0;$$

- *the number of vehicles across the junction is conserved.*

This definition does not ensure uniqueness of the solution, therefore, to get it, we need to select a Riemann Solver at the junction. The choice is made by following ad hoc admissibility criteria, see [8,9].

We recall the definition of Riemann solver at the junction.

Definition 2. *We say that*

$$\mathcal{RS} = (\mathcal{RS}_1, \mathcal{RS}_2, \mathcal{RS}_3) : \Lambda \to \mathrm{BV}(\mathcal{N}; \Lambda), \qquad \Lambda = [0,\rho_{\max}]^3,$$

is a Riemann solver at the junction if for any constant initial datum $\boldsymbol{\rho}_0 = (\rho_{1,0}, \rho_{2,0}, \rho_{3,0}) \in \Lambda$ *the map*

$$(t, \boldsymbol{x}) \mapsto \mathcal{RS}[\boldsymbol{\rho}_0](\boldsymbol{x}/t) = (\mathcal{RS}_1[\boldsymbol{\rho}_0](x_1/t), \mathcal{RS}_2[\boldsymbol{\rho}_0](x_2/t), \mathcal{RS}_3[\boldsymbol{\rho}_0](x_3/t))$$

is a self-similar weak solution to (1)–(2)*,* $h \in \mathsf{H}$*, in the network.*

The self-similar weak solution is obtained by solving three initial boundary value problems

$$\begin{cases} \partial_t \rho_h + \partial_x f_h(\rho_h) = 0, & t > 0,\ x \in \Omega_h, \\ \rho_h(0,x) = \rho_{h,0}, & x \in \Omega_h, \\ \rho_h(t,0) = \rho_{h,b}, & t > 0 \end{cases} \qquad h = 1,\ 2,\ 3. \tag{4}$$

The values $\rho_{h,b}$ are suitable boundary data chosen in order to ensure the conservation at the junction, to produce only waves with negative speed on incoming roads and positive speed on outgoing roads, to satisfy the *consistency property* $\mathcal{RS}[\boldsymbol{\rho}_b] = \boldsymbol{\rho}_b$ and to maximize the passing flow at the junction.

Now, we introduce some notions to select the boundary data maximizing the passing flow at the junction.

Definition 3 (Sect. 5.2.3 in [8]). *For $i \in \mathsf{I}$, the* equilibrium sending capacity *of the i-th incoming road Ω_i is the map $\Delta_i : [0, \rho_{\max}] \to [0, f_i^{\max}]$, see Fig. 1, defined by*

$$\Delta_i(\rho) = \begin{cases} f_i^{\max} & \text{if } \rho \text{ is a good datum,} \\ f_i(\rho) & \text{otherwise.} \end{cases}$$

The equilibrium receiving capacity *of the outgoing road Ω_3 is the map $\Sigma_3 : [0, \rho_{\max}] \to [0, f_3^{\max}]$, see Fig. 1, defined by*

$$\Sigma_3(\rho) = \begin{cases} f_3^{\max} & \text{if } \rho \text{ is a good datum,} \\ f_3(\rho) & \text{otherwise.} \end{cases} \tag{5}$$

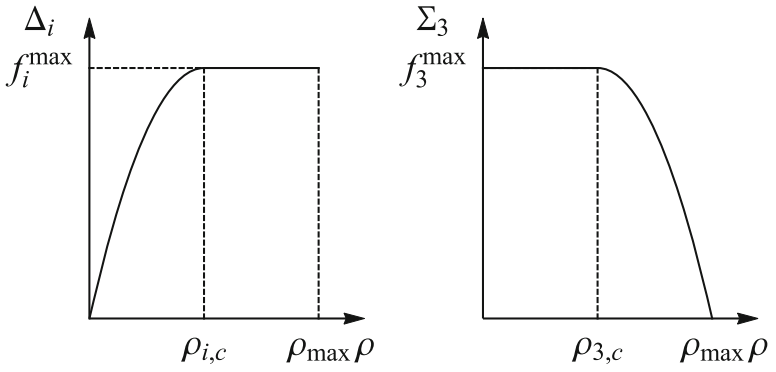

Fig. 1. The equilibrium demand and supply functions.

For the definition of a good and a bad datum, we refer the reader for instance to [8]. The equilibrium receiving represents the maximum flux that an incoming road can demand for a given initial condition, while the equilibrium sending capacity measures the maximum flux that an outgoing road can supply for a given initial condition.

Definition 4. *We fix a priority factor α which has the meaning of a* right of way *and a receiving capacity $Q(\boldsymbol{\rho})$ less than or equal to the equilibrium sending capacity $\Sigma_3(\rho_3)$. We define the* passing flow *at the junction as follows:*

$$\Gamma_1 = \begin{cases} \Delta_1 & \text{if } \Delta_1 + \Delta_2 \le Q, \\ \begin{cases} \Delta_1 & \text{if } \alpha Q \ge \Delta_1, \\ \alpha Q & \text{if } Q - \Delta_2 < \alpha Q < \Delta_1, \\ Q - \Delta_2 & \text{if } \alpha Q \le Q - \Delta_2, \end{cases} & \text{otehrwise} \end{cases} \tag{6}$$

and

$$\Gamma_2 = \begin{cases} \Delta_2 & \text{if } \Delta_1 + \Delta_2 \le Q, \\ Q - \Gamma_1 & \text{otherwise.} \end{cases} \tag{7}$$

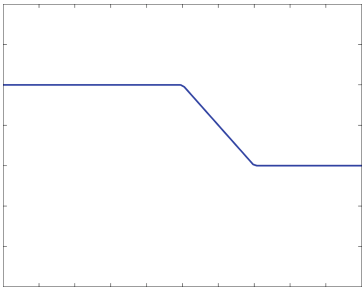

Fig. 2. The qualitative behavior of the constraint function g.

According with the previous rules, we can define the admissible boundary data as

$$\rho_{i,b} = \hat{\rho}_i(\Gamma_i) = \left(f_i\big|_{[\rho_{i,c},\rho_{\max}]}\right)^{-1}(\Gamma_i), \quad i = 1, 2, \tag{8}$$

and

$$\rho_{3,b} = \check{\rho}_3(\Gamma_1 + \Gamma_2) = \left(f_3\big|_{[0,\rho_{3,c}]}\right)^{-1}(\Gamma_1 + \Gamma_2) \tag{9}$$

We can notice that an admissible Riemann solver at the junction $\mathcal{R}_\mathrm{j}$ realizes the maximum of the passing flow at the junction. Indeed, we have

$$\Gamma_1(\boldsymbol{\rho}_0) + \Gamma_2(\boldsymbol{\rho}_0) = \begin{cases} \Delta_1(\rho_{1,0}) + \Delta_2(\rho_{2,0}) & \text{if } \Delta_1(\rho_{1,0}) + \Delta_2(\rho_{2,0}) \le Q(\boldsymbol{\rho}_0), \\ Q(\boldsymbol{\rho}_0), & \text{otherwise.} \end{cases} \tag{10}$$

In order to reproduce the capacity drop phenomenon, we need to introduce a constraint on the junction. We assume that

$$f_3^{\max} < f_1^{\max} + f_2^{\max},$$

then, we define the *constraint function* $g : [0, f_1^{\max} + f_2^{\max}] \to [0, f_3^{\max}]$ in the following way:

$$g(s) = \begin{cases} f_3^{\max} & \text{if } s \le f_3^{\max}, \\ f_3^{\max} + \frac{g_{\min} - f_3^{\max}}{b - f_3^{\max}}\left(s - f_3^{\max}\right) & \text{if } f_3^{\max} < s < b, \\ g_{\min} & \text{otherwise,} \end{cases} \tag{11}$$

where $b \in (f_3^{\max}, f_1^{\max} + f_2^{\max}]$ and $g_{\min} \in (0, f_3^{\max})$.

Figure 2 shows a possible behavior of the constraint function g. The aim of such function is to reduce the outflow through the junction whenever the total sending capacity overcomes the receiving capacity of the outgoing road.

Hence, the non-local model is based on the implementation of the non-local receiving capacity Q^{nl} in the definition of the admissible Riemann Solver, with

$$Q^{nl}(\boldsymbol{\rho}) = \min\left\{\Sigma_3\left(\rho_3(0+)\right), g\left(\Delta_1(\zeta_1) + \Delta_2(\zeta_2)\right)\right\}, \tag{12}$$

where ζ_i is a weighted average of the density of vehicles on Ω_i in a neighborhood of the junction, namely

$$\zeta_i = \int_{-\infty}^{0} w_i(x)\,\rho_i(x)\,\mathrm{d}x,$$

where $w_i \in L^\infty(\mathbb{R}_-;\mathbb{R}_+)$ is an increasing function with compact support in $[-\ell_i, 0]$ and $\|w_i\|_{L^1(\mathbb{R}_-)} = 1$, $i \in \mathsf{I}$.

The admissible Riemann solver here constructed is non-local, as the evaluation of the flow at the junction does not depend on the total sending capacity at the same location, but takes into account a weighted average of the density of vehicles in a left neighborhood of the crossroad. This choice allows for a smooth representation of the transition between the situation in which a capacity drop happens and the case in which the capacity drop is reabsorbed. Additionally, the introduction of a weight function is driven by the fact that in real life the maximum achievable flow at the junction is more affected by the closest densities, while it does not take into account far densities.

In the next section we describe a finite volumes numerical scheme, which can be used to construct a numerical approximation of the solution for the Cauchy problem at a junction with capacity drop representation.

2.2 Finite Volumes Scheme for the Non-local Model

We describe here a constrained numerical method based on the implementation of a finite volume scheme for scalar conservation laws.

We fix a constant space step Δx. For $\ell \in \mathbb{Z}$ and $h \in \mathsf{H}$, we set $x^h_\ell = \ell\Delta x$. We define the cell centers $x^h_{\ell+\frac{1}{2}} = (\ell + \frac{1}{2})\Delta x$ for $\ell \in \mathbb{Z}$ and consider the uniform spatial mesh on each Ω_h

$$\bigcup_{\ell \le -1} [x^i_\ell, x^i_{\ell+1}), \quad i \in \mathsf{I}, \qquad\qquad \bigcup_{\ell \ge 0} [x^3_\ell, x^3_{\ell+1}),$$

so that the position of the junction $x = 0$ corresponds to x^h_0 for each road. Then we fix a constant time step Δt satisfying the CFL condition

$$\Delta t \max_{h\in\mathsf{H}} L_h \le \frac{\Delta x}{2},$$

where L_h is the Lipschitz constant of f_h. For $s \in \mathbb{N}$ we define the time discretization $t^s = s\Delta t$. At each time t^s, $\rho^{h,s}_{\ell+\frac{1}{2}}$ represents an approximation of the mean value of the solution on the interval $[x^h_\ell, x^h_{\ell+1})$, $\ell \in \mathbb{Z}$, along the h-th road.
We initialize the scheme by discretizing the initial conditions

$$\rho^{h,0}_{\ell+\frac{1}{2}} = \frac{1}{\Delta x}\int_{x^h_\ell}^{x^h_{\ell+1}} \rho_{h,0}(x)\ \mathrm{d}x,$$

for all $h \in \mathsf{H}$ and for $\ell \le -1$ if $h \in \mathsf{I}$, $\ell \ge 0$ if $h = 3$.

For each $s \in \mathbb{N}$, at all cell interfaces x_ℓ^h with $\ell \neq 0$, we consider a monotone, consistent numerical flux $F_h(\rho^{h,s}_{\ell-1/2}, \rho^{h,s}_{\ell+1/2})$ corresponding to the flux f_h. At the junction x_0^h we take on each road Ω_h the Godunov flux G_h corresponding to the solution of the Riemann problem at the junction computed by the appropriate solver. We refer the reader to [19] for the definition and basic properties of the Godunov flux.

Then, the finite volumes scheme can be computed by a two-step procedure:

(i) find

$$(\hat\rho_1, \hat\rho_2, \check\rho_3) \text{ such that } \quad f_i(\hat\rho_i) = \Gamma_i \quad \text{for } i \in \mathsf{I} \quad \text{and} \quad f_3(\check\rho_3) = \Gamma_1 + \Gamma_2, \tag{13}$$

where Γ_1 and Γ_2 are defined in (6) and (7);

(ii) compute

$$\rho^{h,s+1}_{\ell+\frac12} = \rho^{h,s}_{\ell+\frac12} - \frac{\Delta t}{\Delta x}\left(\mathcal{F}^{h,s}_{\ell+1} - \mathcal{F}^{h,s}_{\ell}\right), \tag{14}$$

where

$$\mathcal{F}^{h,s}_\ell = \begin{cases} F_h\left(\rho^{h,s}_{\ell-1/2}, \rho^{h,s}_{\ell+1/2}\right) & \text{if } h \in \mathsf{I} \text{ and } \ell \le -1 \quad \text{or} \quad h = 3 \text{ and } \ell \ge 1, \\ G_h\left(\rho^{h,s}_{-\frac12}, \hat\rho_h\right) & \text{if } h \in \mathsf{I} \text{ and } \ell = 0, \\ G_h\left(\check\rho_3, \rho^{h,s}_{\frac12}\right) & \text{if } h = 3 \text{ and } \ell = 0, \end{cases} \tag{15}$$

and $F_h\left(\rho^{h,s}_{\ell-1/2}, \rho^{h,s}_{\ell+1/2}\right)$ is a monotone, consistent numerical flux, i.e. for all $h \in \mathsf{H}$

- F_h is Lipschitz continuous from $[0, \rho_{\max}]^2$ to $\mathbb{R}$,
- $F_h(a, a) = f_h(a)$ for any $a \in [0, \rho_{\max}]$,
- the map $(a, b) \in [0, \rho_{\max}]^2 \mapsto F_h(a, b) \in \mathbb{R}$ is non-decreasing with respect to a and non-increasing with respect to b.

In principle any monotone and consistent numerical flux might be used away from the junction, but we limit our attention to Godunov flux, because all admissible stationary solutions are exact solutions for such scheme.

The step (ii) is a standard marching scheme, while the step (i) is implicit: once per time step, we have to find a zero of a scalar nonlinear function. In our implementation, we compute efficiently the boundary data by using the Regula Falsi method on the interval of definition of the flux function.

Finally, we need to approximate the weighted average of the density ζ_i, $i \in \mathsf{I}$ as follows

$$Z_i^s = \Delta x \sum_{\ell \le 0} w_i(x_{\ell+\frac12}) \rho^{i,s}_{\ell+\frac12}, \qquad i \in \mathsf{I}.$$

In what follows, we present and discuss the numerical results. As we will see, the proposed non-local model is able to represent the capacity drop phenomenon. Moreover, thanks to the study of the observation interval, we can find a way to manage traffic at crossroad in order to distribute vehicles on road network.

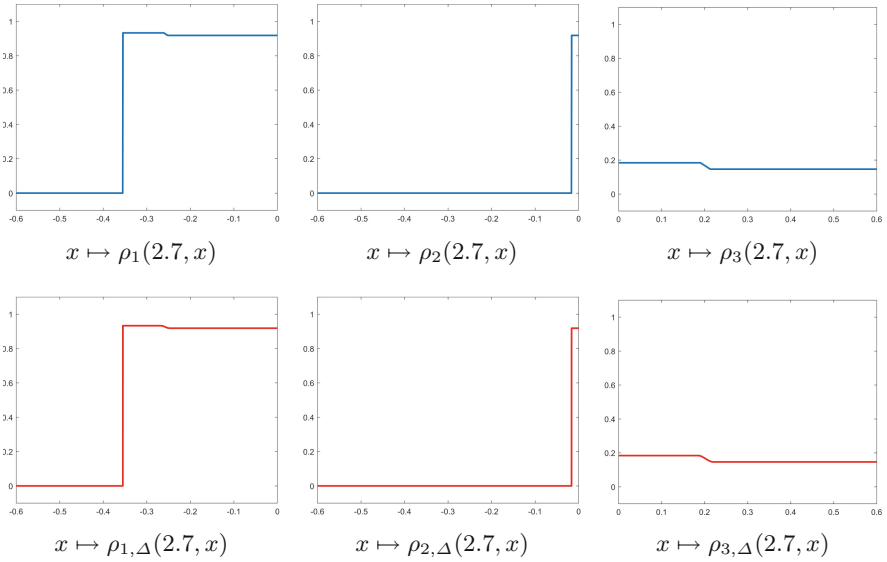

Fig. 3. With reference to the simulation of Sect. 3.1, the comparison between the explicit solution $\boldsymbol{\rho}$ and the numerical one $\boldsymbol{\rho}_\Delta$ at time $t = 2.7$.

3 Numerical Results and Discussion

In this section we validate the implementation of the finite volume scheme presented in the previous section in the constrained setting. The validation of the scheme in the unconstrained case can be found in [19]. The validation consists in a comparison of the numerical approximation with an explicit solution computed in [7].

Additionally, we focus on a comparison between the proposed non-local model and the local one proposed in [10]. In this part we can notice that the capacity drop representation based on non-local point constraint allows to capture a more realistic behavior as the congestion disappears in finite time.

Finally, for a given constraint function g, we discuss the relation between the qualitative behavior of the numerical solution and the choice of the weight function w.

3.1 Validation of the Constrained Method

In order to show that the numerical scheme (13)–(14)–(15) is able to integrate in a coherent way the non-local point constraint at the junction, we validate it by comparison with the explicit solution computed in [7].

The parameters for the simulation are $\Delta x = 0.5 \times 10^{-4}$ and $\Delta t = 0.25 \times 10^{-4}$.

In Fig. 3 we compare the numerical and the explicit solution at time $t = 2.7$. We observe a good agreement of these profiles. We perform a convergence

analysis for this test. We introduce the relative L^1-error respectively for the whole network, for the incoming and for the outgoing roads at a given time t^s as follows

$$E_{L^1}^{s,\mathcal{N}} = \frac{\sum_{h=1}^{3}\sum_{\ell}|\rho_h(t^s,x_\ell)-\rho_\ell^{h,s}|}{\sum_{h=1}^{3}\sum_{\ell}|\rho_h(t^s,x_\ell)|},$$
$$E_{L^1}^{s,\mathrm{I}} = \frac{\sum_{h=1}^{2}\sum_{\ell}|\rho_i(t^s,x_\ell)-\rho_\ell^{i,s}|}{\sum_{i=1}^{2}\sum_{\ell}|\rho_i(t^s,x_\ell)|},$$
$$E_{L^1}^{s,3} = \frac{\sum_{\ell}|\rho_3(t^s,x_\ell)-\rho_\ell^{3,s}|}{\sum_{\ell}|\rho_3(t^s,x_\ell)|}.$$

Table 1 depicts the relative L^1-error with respect to the space step at the fixed time $t = 2.7$. We observe that the rate of convergence is approximately 1. This means that the introduction of a non-local point constraint does not affect the accuracy of the scheme.

Table 1. Relative L^1-error at time $t = 2.7$ computed in Sect. 3.1

Number of cells per road	$E_{L^1}^{s,\mathcal{N}}$	Rate of convergence	$E_{L^1}^{s,\mathrm{I}}$	Rate of convergence	$E_{L^1}^{s,3}$	Rate of convergence
60	3.0860×10^{-2}	–	3.0882×10^{-2}	–	3.0783×10^{-2}	–
120	2.4713×10^{-2}	0.3205	2.7028×10^{-2}	0.1923	1.6441×10^{-2}	0.9048
600	5.4311×10^{-3}	0.7874	5.6482×10^{-3}	0.7792	4.6523×10^{-3}	0.8143
1200	2.6768×10^{-3}	0.8442	2.6246×10^{-3}	0.8565	2.8639×10^{-3}	0.7909
6000	9.3434×10^{-4}	0.8024	9.4064×10^{-4}	0.8115	9.1174×10^{-4}	0.7612
12000	5.8915×10^{-4}	0.7816	6.0521×10^{-4}	0.7867	5.3150×10^{-4}	0.7560

3.2 Local and Non-local Constrained Method at the Junction

We make a numerical comparison between the proposed non-local model and the local one proposed in [10].

As explained in the previous sections, local methods can suffer of the lack of consistency, and as a consequence the stationary solutions are not fixed points for the associated Riemann solver. Moreover, a local approach in suitable cases is not able to recover a traffic jam after that a capacity drop happens.

We perform a simulation analogous to the one made in [10]. We parametrize the incoming roads by the segment $[-12/5, 0]$ and the outgoing road by $[0, 12/5]$. We take

$$f(\rho) = \frac{9}{4 \cdot 10^6 \sqrt{5}}\, \rho \left(10^4 - \rho^2\right)^2,$$

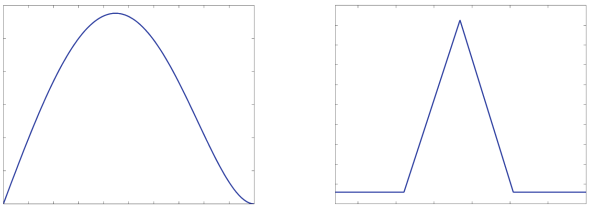

$\rho \mapsto f(\rho)$ $\qquad$ $x \mapsto \rho_{1,0}(x)$

Fig. 4. Flux and initial condition on the first incoming road considered in Sect. 3.2.

as flux for each road, see Fig. 4 on the left. As initial conditions, see Fig. 4 on the right, we fix

$$\rho_{1,0}(x) = \begin{cases} p_1 & \text{if } x \le x_1, \\ p_1 + \frac{p_2 - p_1}{x_2 - x_1}(x - x_1) & \text{if } x_1 < x \le x_2, \\ p_1 - \frac{p_2 - p_1}{x_3 - x_2}(x - x_3) & \text{if } x_2 < x \le x_3, \\ p_1 & \text{if } x_3 < x \le 0, \end{cases} \qquad \rho_{2,0} = p_1, \quad \rho_{3,0} = p_3,$$

where

$$p_1 = 14.5190, \qquad p_2 = 16.2511, \qquad p_3 = 38.0366,$$
$$x_1 = -2.3957, \qquad x_2 = -1.6588, \qquad x_3 = -0.9583.$$

We take

$$g(s) = \begin{cases} 2880 & \text{if } 0 \le s \le 2880, \\ 5760 - s & \text{if } 2880 < s < 3024, \\ 2736 & \text{if } 3024 \le s \le 5760, \end{cases}$$

as constraint function, and we choose the weight function $w(x) = 2(1 + x)\chi_{[-1,0]}(x)$. The parameters for the simulation are $\Delta x = 10^{-4}$, $\Delta t = (\sqrt{5}/45) \times 10^{-5}$ and $\alpha = 1/2$.

We compute and compare the approximate solutions corresponding to the local and the non-local model.

Figure 5 shows that, as observed in [10], even if the initial condition leads to a moderate congestion, the shock in the solution corresponding to the local model is never reabsorbed. On the other hand, the non-local model allows the congestion to be reabsorbed in finite time.

Figure 6 shows the dynamic of the shocks on Ω_1 in the solution corresponding to the local and the non-local model. On the x-axis we represent time and on the y-axis we represent the distance from the junction. We can observe that the non-local approach allows the traffic jam to disappear at a smoothly increasing rate while with the other approach the congestion keeps growing forever.

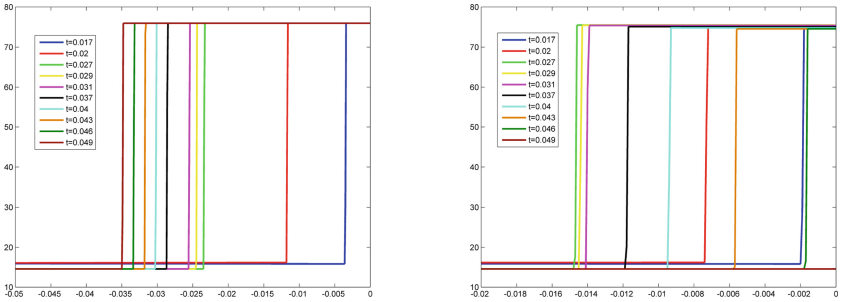

Fig. 5. With reference to Sect. 3.2. Left panel: The zoom of the profiles of solution on Ω_1 corresponding to the local model under consideration in a neighborhood of the junction as time evolves. Right panel: The zoom of the profiles of solution on Ω_1 corresponding to the non-local model in a neighborhood of the junction as time evolves.

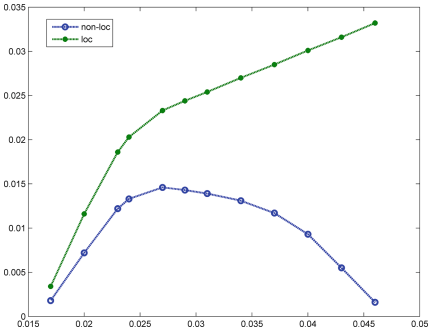

Fig. 6. With reference to Sect. 3.2, the dynamic of the shocks on Ω_1 in the solution corresponding to the local and the non-local model.

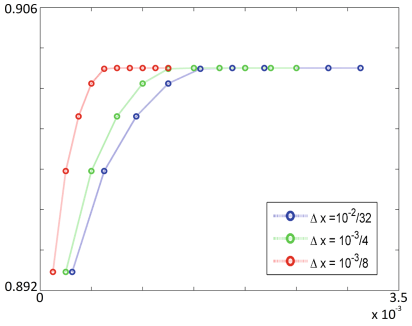

Fig. 7. With reference to Sect. 3.2, the changing of the value of the boundary datum on Ω_1 when the local Riemann solver is iterated.

Finally, we prove numerically that the local model proposed in [10] is not consistent. The lack of consistency means that the Riemann Solver provides not stable solutions. As a consequence, if we implement the solver in a finite volumes numerical scheme we do not observe the expected solution as it is destroyed after few iterations. Figure 7 plots the boundary value $\hat{\rho}_{1,b}$ of the first incoming road as time evolves for different space step. We can observe that after few iterations the method stabilizes itself around a value different by the boundary datum provided by the local solver.

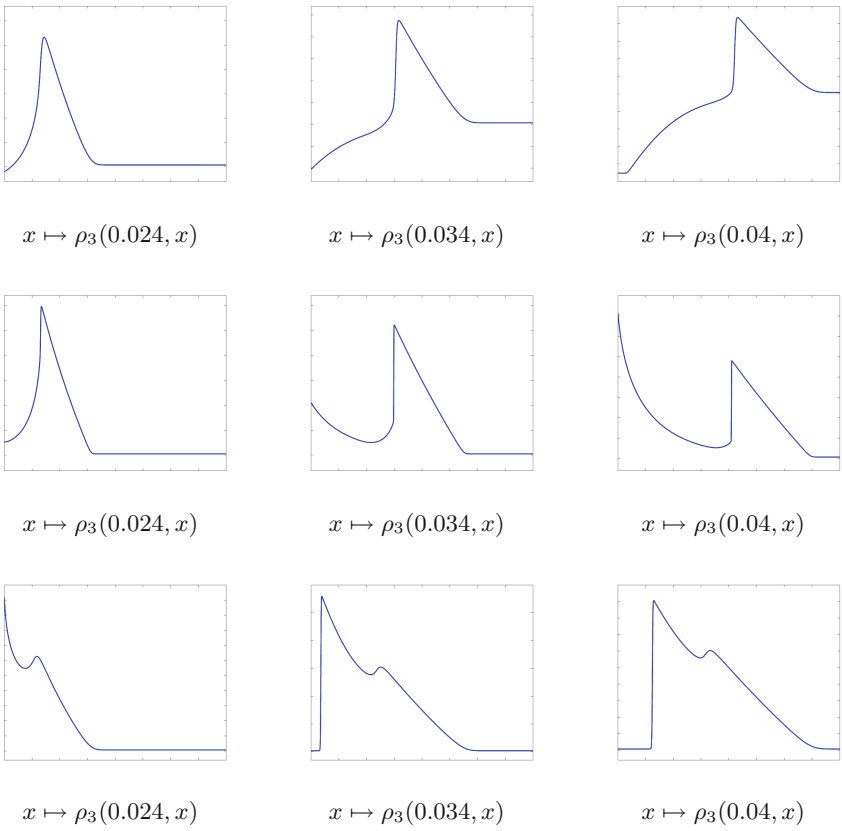

Fig. 8. With reference to Sect. 3.3, the profiles of the solution on Ω_3 with varying observation interval $\mathrm{supp}(w)$: in the first line $\mathrm{supp}(w) = [-0.98, 0]$, in the second line $\mathrm{supp}(w) = [-1, 0]$, in the last line $\mathrm{supp}(w) = [-1.2, 0]$.

3.3 Qualitative Behavior of the Solutions with Respect to the Observation Interval

We investigate, here, the role of the weight function w. To do this, we run simulations using the same setting and data as before, but letting the support of w vary.

We plot in Fig. 8 the profiles of the solutions on the outgoing road Ω_3 corresponding to $\min\{\text{supp}(w)\} \in \{-1.2, -1, -0.98\}$.

We find that the behavior of the solution changes continuously depending on the value of $\min\{\text{supp}(w)\}$. In particular, the first line shows that the capacity of the junction diminishes gradually, but the congestion last forever as in the local model. In the second line we can observe a capacity recovery after the capacity drop. This fact might be interpreted by a sort of "self-organization" strategy of the vehicles. In the last line the capacity drop becomes so small that it practically does not have any impact on the behavior of the solution.

Such result represents an important aspect in order to propose response strategies able to manage traffic near crossroads and to avoid traffic jams.

The peculiarity of the proposed non-local model relies in the possibility to let the observational interval to vary depending on the vehicles averaged density in order to limit the capacity drop phenomenon. This aspect could help drivers to choice the best route from their present location.

For instance, such result can be used to calibrate the parameters of the model and to positioning traffic sensors more efficiently.

4 Conclusions

In this paper, in the framework of smart cities, we propose a non-local constrained model and a finite volume scheme to reproduce the capacity drop phenomenon at a road merge. Our simulations show that the model converges numerically and is able to suggest a strategy to manage traffic at crossroads. Indeed, thanks to the implementation of a non-local model, we are able to provide more accurate results from sensors data revelation, which can take into account not only point values, but average values in suitable observational interval. The determination of the size of such interval and the best location of sensors in this new setting can be done by calibrating the parameters of the model with real traffic data. This represents a further step we intend to investigate to improve our results.

Acknowledgements. This paper has been supported by GNCS of Istituto Nazionale di Alta Matematica, by PRIN 2017 "Discontinuous dynamical systems: theory, numerics and applications" and by Regione Puglia, "Programma POR Puglia 2014/2020-Asse X-Azione 10.4 Research for Innovation-REFIN - (D1AB726C)".

References

1. Albi, G., Cristiani, E., Pareschi, L., Peri, D.: Mathematical models and methods for crowd dynamics control. In: Gibelli, L. (ed.) Crowd Dynamics, Volume 2. MSSET, pp. 159–197. Springer, Cham (2020). https://doi.org/10.1007/978-3-030-50450-2_8
2. Andreianov, B., Donadello, C., Razafison, U., Rosini, M.D.: Qualitative behaviour and numerical approximation of solutions to conservation laws with non-local point constraints on the flux and modeling of crowd dynamics at the bottlenecks. ESAIM: Math. Model. Numer. Anal. **50**(5), 1269–1287 (2016). https://doi.org/10.1051/m2an/2015078
3. Caragliu, A., Del Bo, C., Nijkamp, P.: Smart cities in Europe. J. Urban Technol. **18**(2), 65–82 (2011). https://doi.org/10.1080/10630732.2011.601117
4. Chiou, S.-W.: A data-driven traffic-responsive signal control for a smart city road network under uncertainty. In: García Márquez, F.P., Lev, B. (eds.) Introduction to Internet of Things in Management Science and Operations Research. ISORMS, vol. 311, pp. 119–146. Springer, Cham (2021). https://doi.org/10.1007/978-3-030-74644-5_6
5. Coclite, G.M., Fanizzi, A., Lopez, L., Maddalena, F., Pellegrino, S.F.: Numerical methods for the nonlocal wave equation of the peridynamics. Appl. Numer. Math. **155**, 119–139 (2020). https://doi.org/10.1016/j.apnum.2018.11.007
6. Coclite, G.M., Paparella, F., Pellegrino, S.F.: On a salt fingers model. Nonlinear Anal. **176**, 100–116 (2018). https://doi.org/10.1016/j.na.2018.06.007
7. Dal Santo, E., Donadello, C., Pellegrino, S.F., Rosini, M.D.: Representation of capacity drop at a road merge via point constraints in a first order traffic model. ESAIM: Math. Model. Numer. Anal. **53**(1), 1–34 (2019). https://doi.org/10.1051/m2an/2019002
8. Garavello, M., Piccoli, B.: Traffic flow on networks. In: AIMS Series on Applied Mathematics, vol. 1. MO, American Institute of Mathematical Sciences (AIMS), Springfield (2006)
9. Garavello, M., Piccoli, B.: Conservation laws on complex networks. Annales de l'Institut Henri Poincare (C) Non Linear Analysis **26**(5), 1925–1951 (2009). https://doi.org/10.1016/j.anihpc.2009.04.001
10. Haut, B., Bastin, G., Chitour, Y.: A macroscopic traffic model for road networks with a representation of the capacity drop phenomenon at the junctions. In: Proceedings 16th IFAC World Congress, Prague, Czech Republic. vol. 229, pp. Tu-M01-TP/3 (2005)
11. Lighthill, M.J., Whitham, G.B.: On kinematic waves. II. A theory of traffic flow on long crowded roads. Proc. Roy. Soc. London. Ser. A. **229**, 317–345 (1955). https://doi.org/10.1098/rspa.1955.0089
12. Liu, C., Ke, L.: Cloud assisted Internet of things intelligent transportation system and the traffic control system in the smart city. J. Control Decis. 1–14 (2022). https://doi.org/10.1080/23307706.2021.2024460
13. Lopez, L., Pellegrino, S.F.: A space-time discretization of a nonlinear peridynamic model on a 2D lamina. Comput. Math. with Appl. **116**, 161–175 (2022). https://doi.org/10.1016/j.camwa.2021.07.004
14. Lopez, L., Pellegrino, S.F.: A spectral method with volume penalization for a nonlinear peridynamic model. Int. J. Numer. Meth. Eng. **122**(3), 707–725 (2021). https://doi.org/10.1002/nme.6555
15. Lopez, L., Pellegrino, S.: Computation of eigenvalues for nonlocal models by spectral methods. J. Peridyn. Nonlocal Model. (2021). https://doi.org/10.1007/s42102-021-00069-8

16. Masek, P., et al.: A harmonized perspective on transportation management in smart cities: the novel IoT-driven environment for road traffic modeling. Sensors **16**(11), 1872 (2016). https://doi.org/10.3390/s16111872
17. Ngoduy, D.: Noise-induced instability of a class of stochastic higher order continuum traffic models. Transp. Res. B: Methodol. **150**, 260–278 (2021). https://doi.org/10.1016/j.trb.2021.06.013
18. Papamichail, I., Papageorgiou, M.: Traffic-responsive linked ramp-metering control. IEEE Trans. Intell. Transp. Syst. **9**(1), 111–121 (2008). https://doi.org/10.1109/TITS.2007.908724
19. Pellegrino, S.F.: On the implementation of a finite volumes scheme with monotone transmission conditions for scalar conservation laws on a star-shaped network. Appl. Numer. Math. **155**, 181–191 (2020). https://doi.org/10.1016/j.apnum.2019.09.011
20. Pellegrino, S.F.: Simulations on the peridynamic equation in continuum mechanics. In: Skiadas, C.H., Dimotikalis, Y. (eds.) CHAOS 2020. SPC, pp. 635–649. Springer, Cham (2021). https://doi.org/10.1007/978-3-030-70795-8_46
21. Richards, P.I.: Shock waves on the highway. Oper. Res. **4**, 42–51 (1956). https://doi.org/10.1287/opre.4.1.42
22. Torrisi, V., Ignaccolo, M., Inturri, G.: Analysis of road urban transport network capacity through a dynamic assignment model: validation of different measurement methods. Transp. Res. Procedia **27**, 1026–1033 (2017). https://doi.org/10.1016/j.trpro.2017.12.135, 20th EURO Working Group on Transportation Meeting, EWGT 2017, 4–6 September 2017, Budapest, Hungary
23. Willis, K., Aurigi, A.: The Routledge Companion to Smart Cities. Routledge, Taylor & Francis Group (2020)